Longitudinal Synchrotron Beam-Pulse Shapes

Hermann Meuth
Forschungszentrum Jülich GmbH
Postfach 1913, D-5170 Jülich

Abstract

A general analytical expression for current waveforms of the longitudinal particle-beam pulse (i.e. the line density) in a synchrotron is derived for an arbitrary particle distribution in canonical phase space, that is a function of the Hamiltonian alone. Pertinent bucket parameters, as synchronous phase angle, and bucket filling enter. In principle, this approach permits to also treat the inverse problem, by which the phase space distribution may be inferred from a known (e.g. measured) beam-pulse waveform. In model examples, the beam-pulse waveforms' center-of-charge phase, and their fundamental (h=1) phase are compared with the synchronous phase for a harmonic rf voltage. While the former two phase values differ only slightly, there is a considerable discrepancy between them, and the synchronous phase, even at only moderate bucket fillings, and moderate acceleration. This entails, in effect, a sizeable, time varying phase slip during an acceleration ramp from injection to top energy, if no synchrotron-phase control loop is employed.

1. PREREQUISITES

Let the rf bucket be characterized by the Hamiltonian in reduced form, see Dôme [1], whose notation will largely be followed:

$$H^* = \frac{y^2}{2} - \Psi(\phi) = \frac{y^2}{2} - \mathrm{sgn}(\eta)\,[\Gamma\phi + G(\phi)] \quad , \qquad (1)$$

where the parameter η is defined such that, $\eta > 0$ below the gamma transition, i.e. $\eta = \gamma^{-2} - \gamma_{tr}^{-2}$. The quantity $-\Psi(\phi)$ constitutes the "potential" term in the Hamiltonian (1). In the stationary and adiabatically time variant case, beam particles move along phase trajectories, determined by $H^* = C$, i.e. by the family of curves $y(C,\phi) = \sqrt{\{2[C+\Psi(\phi)]\}}$, or

$$y(C,\phi) = \sqrt{2}\,\sqrt{C + \mathrm{sgn}(\eta)\,[\Gamma\phi + G(\phi)]} \quad . \qquad (2)$$

More precisely, $y(C,\phi)$ is defined as the real part of the R.H.S. of (2), *vanishing for negative definite expressions under the root.* Let us suppose now, that the beam particles populating the phase space region delimited by the interval $[C,C+\Delta C]$ have the (equilibrated) density $\rho(C)$. While the potential $-\Psi(\phi)$ is a property of the bucket, $\rho(C)$ is clearly a particle property.

To determine the beam-pulse waveform, we seek the projection of this density $\rho(C)$ onto the phase (or s-, or time-) axis, as schematically shown in Fig. 1. The number of all particles enclosed by the intervals $[C,C+\Delta C]$ and $[\phi,\phi+\Delta\phi]$ is $F(\phi)\,\Delta\phi = \Sigma_i \rho(C_i)\Delta y(C_i,\phi)\,\Delta\phi$, defining the projected density

$$F(\phi) = \int_{C_{min}}^{C_{max}} dC\, \rho(C)\, \frac{\partial y(C,\phi)}{\partial C} \quad , \qquad (3)$$

by expanding $\Delta y(C_i,\phi) = y(C_i+\Delta C,\phi) - y(C_i,\phi)$ of Fig. 1.

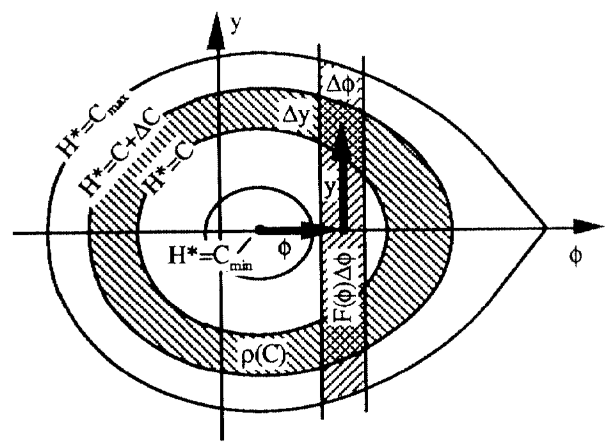

Fig. 1: Schematic depiction of longitudinal phase space

The integration limits in Equ. (3), C_{min} and C_{max}, follow from the condition that a stable phase space distribution $\rho(C)$ exist, i.e. from the stable and unstable potential points, respectively,

$$\left[\frac{\partial H^*}{\partial \phi}\right]_{C=C_{min}} = \left[\frac{\partial H^*}{\partial \phi}\right]_{C=C_{max}} = 0 \quad , \qquad (4)$$

from which, in turn, will result, the conditions for ϕ_{min} and ϕ_{max}, i.e. $\Psi(\phi_{min/max})' = \Gamma + G'(\phi_{min/max}) = 0$. With these, we arrive at C_{min} and C_{max}

$$\begin{aligned} C_{min/max} &= -\Psi(\phi_{min/max}) \\ &= -\,\mathrm{sgn}(\eta)\,[\Gamma\phi_{min/max} + G(\phi_{min/max})] \,. \end{aligned} \qquad (5)$$

In Fig. 2, the potential functions of the bucket, $-\Psi(\phi)$, for $\eta<0$ and $\eta>0$ are depicted. Also, examples of phase space densities $\rho(C)$ are shown schematically.

Now, for a harmonic rf voltage, Γ and $G(\phi)$ become $\Gamma = \sin\phi_s$ and $G(\phi) = \cos\phi$. Consequently, from Equ. (5), the relation $\sin\phi_s = \sin\phi_{min/max}$ must hold for both ϕ_{min} and ϕ_{max}, whence we get $\phi_{min} = \phi_s$ and $\phi_{max} = \phi_u = \pi - \phi_s$. To clarify our notation: the phase values $\phi_{min} = \phi_s$ and $\phi_{max} = \phi_u$ ($=\pi-\phi_s$ for harmonic rf) correspond to the minimum and maximum *potential* value C_{min}, and C_{max}, respectively. In contrast, the smallest (for $\eta>0$), or largest (for $\eta<0$) attainable *phase* value, ϕ_e, follows from the second solution within the bucket of Equ. (5) for $C=C_{max}$, $\phi=\phi_{max}=\phi_u$ (cf. Fig. 2):

$$C_{max} = -\,\mathrm{sgn}(\eta)\,[\Gamma\phi_u + G(\phi_u)] = -\,\mathrm{sgn}(\eta)\,[\Gamma\phi_e + G(\phi_e)]. \quad (6)$$

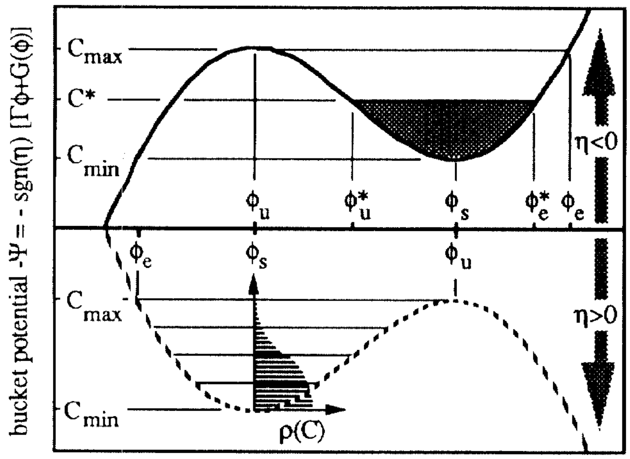

phase ϕ

Fig. 2: Potential functions versus phase for $\eta>0$ and $\eta<0$

With the specific square-root form of $y(C,\phi)$ [Equ. (2)], or via partial integration, the projected density distribution $F(\phi)$ [Equ. (3)] may be re-expressed as

$$F(\phi) = \int_{C_{min}}^{C_{max}} dC\,\frac{\rho(C)}{y(C,\phi)} = -\int_{C_{min}}^{C_{max}} dC\,\frac{d\rho(C)}{dC}\,y(C,\phi) + \rho(C)y(C,\phi)\Big|_{C_{max}} . \quad (7)$$

Since $y(C_{min},\phi)\equiv 0$, the lower limit product on the R.H.S. disappeared. For the upper limit product one must observe that the limit condition for $\rho(C_{max}+\varepsilon)\equiv 0$ *outside* the bucket holds for stability reasons, but a finite limit value *inside* the bucket is allowed, i.e. $\lim_{\varepsilon\to 0}\rho(C_{max}-\varepsilon)\neq 0$.

The extrema of $F(\phi)$ occur subject to the condition $\partial y/\partial\phi=0$, or $\Gamma+G'(\phi)=0$, and thus at the phase values ϕ_s, ϕ_u, and ϕ_e. For the first, $F(\phi)$ has a maximum, $F(\phi_s)$, while minima for ϕ_u, and ϕ_e (or, at least, edge minima).

Once the distribution $F(\phi)$ is in hand, a number of relevant quantities may be computed in terms of moments of $F(\phi)$. Denoting the n^{th} moment by

$$\langle\phi^n\rangle = \int_{-\pi}^{\pi} d\phi\,\phi^n\,F(\phi) \quad , \quad (8)$$

the norm of F would be $\langle 1\rangle$. The average phase angle is then $\phi_c=\langle\phi\rangle/\langle 1\rangle$, describing the beam pulse's center of charge (in radians). On the other hand, the phase of the h^{th} harmonic of the waveform is computed from the Fourier decomposition, $\phi_h=\mathrm{arctg}\{\langle\sin(h\phi)\rangle/\langle\cos(h\phi)\rangle\}$. The duty cycle may be defined as $T=\langle 1\rangle/[2\pi F(\phi_s)]$, while the root-mean square deviation, $\Delta\phi_{rms}=\sqrt{\{[\langle\phi^2\rangle-\langle\phi\rangle^2]/\langle 1\rangle\}}$, would be a measure for the beam-particle pulse width (or length, in radians). A different, yet also common measure for the pulse width is the difference $\Delta\phi_v=\phi_{fall}-\phi_{rise}$, with $\phi_{rise,fall}$ following from the fraction ν (say, e.g. $\nu=0.1$) via $F(\phi_{rise})/F(\phi_s)=F(\phi_{fall})/F(\phi_s)=\nu$.

2. Specific Phase Space Densities $\rho(C)$

To get an impression of possible projected distributions $F(\phi)$ following from Equ. (7), a specific phase space density distribution $\rho(C)$ has to be assumed. For its simplicity, we first choose a rectangular distribution, i.e. a distribution $\rho(C)$ that is constant up to a certain point $C=C^*$, dropping thereafter abruptly to zero. Subsequently, the general case is treated, where $\rho(C)$ is allowed to be any power series of arbitrary order in C, for which the resulting $F(\phi)$ is given explicitly, again in terms of a power series. As an example for this general result, the results for a triangular, and a parabolic distribution are presented. Finally, the possibilities for an inverse approach are discussed.

2.1. Rectangular (Constant) Density Distribution

We set $\rho(C)=1$ for $C_{min}\leq C\leq C^*$, and $\rho(C)=0$ for $C^*<C\leq C_{max}$. In Fig. 2, the various limit quantities of C and ϕ are clarified in an example for $\eta<0$. In this simple case, the projected density $F(\phi)$ of Equ. (3) turns into a complete integral, $F(\phi) = y(C^*,\phi)$. The density $F(\phi)$ is real, and therefore non-zero only for the range $\phi_e^*\leq\phi\leq\phi_u^*\leq\phi_{max}$ (for $\eta>0$), and $\phi_e^*\geq\phi\geq\phi_u^*\geq\phi_{max}$ (for $\eta<0$). We may introduce a fill fraction μ, such that the "fill level" in the bucket is at $\mu\times$(maximum bucket *height*) to get $C^*=\mu C_{max}+(1-\mu)C_{min}$. (Different definitions for the fill fraction according to bucket *area* or *volume* are also conceivable.) Substituting for C_{min} and C_{max} from Equ. (6) results in the general value C^* or, respectively, in the value C^* for harmonic rf voltage,

$$\begin{aligned} C^* &= -\mathrm{sgn}(\eta)\,\{[\mu\phi_u+(1-\mu)\phi_s]\Gamma + \mu G(\phi_u) + (1-\mu)G(\phi_s)\} \\ &= -\mathrm{sgn}(\eta)\,\{[\mu\pi + (1-2\mu)\phi_s]\sin\phi_s + (1-2\mu)\cos\phi_s\}\ , \end{aligned} \quad (9)$$

and finally, with Equ. (2), in the projected distribution

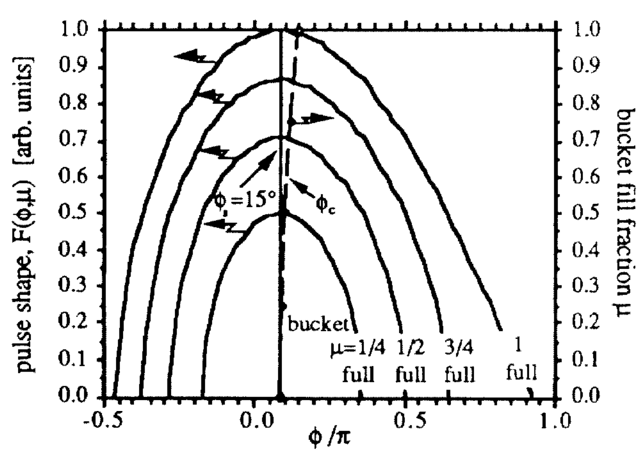

Fig. 3: Line density waveforms for various bucket filling

$$F(\phi,\mu) = \sqrt{2\,\mathrm{sgn}(\eta)\{[\phi-(1-2\mu)\phi_s-\mu\pi]\sin\phi_s+\cos\phi-(1-2\mu)\cos\phi_s\}} \quad (10)$$

omitting the general rf case for brevity; it follows directly from Equs. (2) and (9). In Fig. 2, the levels of C^* for $\mu=1$, $\mu=3/4$, $\mu=1/2$ and $\mu=1/4$ were shown schematically for $\eta>0$. In Fig. 3, the projected distribution $F(\phi,\mu)$ is depicted for these four fill factors μ, for a synchronous phase of $\phi_s = 15°$. We observe that the pulse center of charge ϕ_c, and the phase of the fundamental, $\phi_{h=1}$, are shifted away from ϕ_s to higher values for increasing bucket fill fraction μ, which is shown in more detail in Fig. 4.

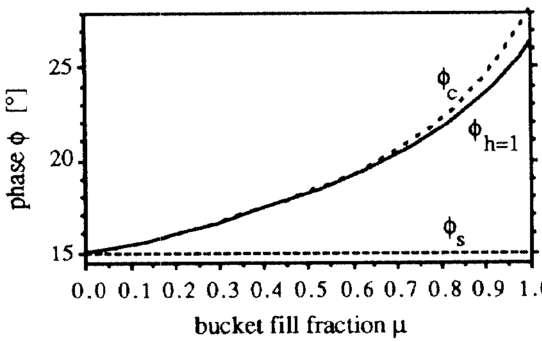

Fig. 4: Synchronous, center-of-mass, and fundamental phase

2.2. Arbitrary Density Distribution

For the general case of an *arbitrarily variable* density $\rho(C)$ we only shall assume, that $\rho(C)$ is given in form of an arbitrary power series in $C-C_{min}$:

$$\rho(C) = \sum_{n=0}^{\infty} \rho_n (C - C_{min})^n \quad (11)$$

With it, and with $F(\phi,\mu=1)=y(C_{max},\phi)$ [Equ. (2) for $C=C_{max}$], which is not restricted to harmonic rf, we get for the projected distribution from Equ. (7):

$$F(\phi) = -\frac{1}{2} F(\phi,1)^3 \times \sum_{n=0}^{\infty} (n+1)\, \rho_{n+1}\, I_n(\phi) + F(\phi,1)\, \rho(C_{max}) \,. \quad (12)$$

The integrals $I_n(\phi)=2F(\phi,1)^{-3}\int dC[(C-C_{min})^n y(C,\phi)]$ are evaluated by binomial expansion,

$$I_n(\phi) = \sum_{k=0}^{n}\sum_{l=0}^{n-k}\sum_{m=0}^{k} \frac{(-1)^{n-k}}{k+\frac{3}{2}} \binom{n}{k}\binom{n-k}{l}\binom{k}{m} C_{max}^{k-m}\, C_{min}^{n-k-l}\, \Psi(\phi)^{l+m} \,. \quad (13)$$

with $\Psi(\phi)$ following from Equ. (1), and $C_{max/min}$ from Equ. (5).

2.3. Examples: Linear and Parabolic Density Distribution

The constant density of Sect. 2.1 is of course a special case of Equ. (11) for $\rho_0\neq 0$, $\rho_{n\neq 0}=0$. The next simplest case of expansion (11) is a phase space distribution $\rho(C)$ which drops linearly in C, i.e. $\rho(C)=1-(C-C_{min})/(C_{max}-C_{min})$; all $\rho_{n>1}$ vanish. Since $\rho(C_{max}-C_{min})=0$, the second term on the R.H.S. of Equ. (12) disappears, while the only non-zero integral is $I_0(\phi)=1/3$, independent of ϕ. Thus (disregarding an unessential normalization constant)

$$F_\Delta(\phi) = F(\phi,1)^3 \,, \quad (14)$$

Now we consider the case $\rho(C)=1-[(C-C_{min})/(C_{max}-C_{min})]^2$, i.e. a parabolically varying distribution, with $\rho_1=0$, $\rho_{n>2}=0$. Here, $I_1(\phi)=\mathrm{sgn}(\eta)[(5\phi_s-3\phi_u-2\phi)\Gamma+5G(\phi_s)-3G(\phi_u)-2G(\phi)]/15$. Again aside from a constant, the pulse shape becomes then

$$F_\cap(\phi)=F(\phi,1)^3\,\mathrm{sgn}(\eta)[(5\phi_s-3\phi_u-2\phi)\Gamma+5G(\phi_s)-3G(\phi_u)-2G(\phi)] \quad (15)$$

For harmonic rf, both the shapes of $F_\Delta(\phi)$ and $F_\cap(\phi)$ [i.e. for "triangular" (linear), and "parabolic" $\rho(C)$] are compared with the "constant" case for $\mu=1$ from Equ. (10) above.

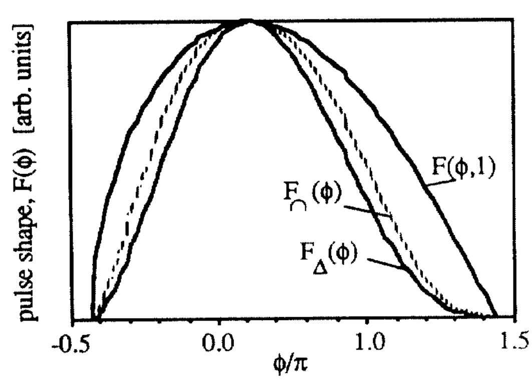

Fig. 5: Line density for simple distributions $\rho(C)$

For $\phi_s=15°$, one obtains the phase values $\phi_{h=1}=20.24°$, and $\phi_c=21.03°$ (Δ) and $\phi_{h=1}=21.23°$, and $\phi_c=22.09°$ ($\cap$), which are to be compared with Fig. 4.

2.4. The Inverse Problem

So far, we *assumed* a phase space density $\rho(C)$ to arrive at the line density $F(\phi)$. Of diagnostic interest is, however, the reversed situation, since the line density can be *measured.* For this objective, a numerical approach has recently been proposed, [2] although restricted to elliptic phase space contours (i.e. a small phase angle or harmonic limit).

If we assume that $\rho(C)$ goes smoothly to zero, as C approaches C_{max}, then the second term on the R.H.S. of Equ. (12) vanishes. The remaining sum $\Sigma(n+1)\rho_{n+1}I_n(\Psi)$ constitutes an expansion in the polynomials $I_n(\Psi)$ of order Ψ^n. Thus, these polynomials are linearly independent, which is necessary for putting an inverse procedure on mathematically sound footing. Therefore, from the "reduced" beam pulse shape $F(\phi)/F(\phi,1)^3$, we can, at least in principle, determine uniquely the expansion coefficients $(n+1)\rho_{n+1}/2$ to the polynomials $I_n(\Psi)$, to find $\rho(C)$ from Equ. (11), to within one (arbitrary) normalization constant ρ_0.

3. REFERENCES

[1] G. Dôme, CAS '85, CERN 87-03, p. 110

[2] Joseph M. Kats, PAC 1991, San Francisco